Pound-locking for characterization of superconducting microresonators

T. Lindström, J. Burnett, M. Oxborrow, and A Ya. Tzalenchuk

View Online   **Export Citation**

ARTICLES YOU MAY BE INTERESTED IN

Planar superconducting resonators with internal quality factors above one million
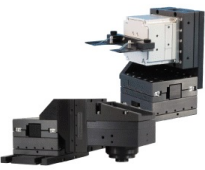Applied Physics Letters **100**, 113510 (2012); https://doi.org/10.1063/1.3693409
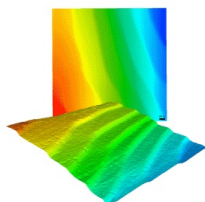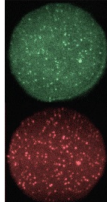
Reducing intrinsic loss in superconducting resonators by surface treatment and deep etching
of silicon substrates
Applied Physics Letters **106**, 182601 (2015); https://doi.org/10.1063/1.4919761

A quantum engineer's guide to superconducting qubits
Applied Physics Reviews **6**, 021318 (2019); https://doi.org/10.1063/1.5089550

Nanopositioning
Systems

Modular
Motion Control

AFM and NSOM
Instruments

Single Molecule
Microscopes

MCL
MAD CITY LABS INC.
www.madcitylabs.com

AIP
Publishing

Pound-locking for characterization of superconducting microresonators

T. Lindström,[1,2] J. Burnett,[1,2] M. Oxborrow,[1] and A Ya. Tzalenchuk[1]
[1]*National Physical Laboratory, Hampton Road, Teddington TW11 0LW, United Kingdom*
[2]*Royal Holloway, University of London, Egham Hill, Egham TW20 0EX, United Kingdom*

We present a new application and implementation of the Pound-locking technique for the interrogation of superconducting microresonators. We discuss how by comparing against stable frequency sources this technique can be used to characterize properties of resonators that cannot be accessed using traditional methods. Specifically, by analyzing the noise spectra and the Allan deviation, we obtain valuable information about the nature of the noise in superconducting planar resonators. This technique also greatly improves the read-out accuracy and measurement throughput compared to conventional methods. [doi:10.1063/1.3648134]

I. INTRODUCTION

Resonators are ubiquitous devices used in one form or another in most areas of physics and in many important applications, from filters in mobile phones to experiments in cavity quantum electrodynamics.[1] Over the past few years, advances in on-chip quantum information processing have meant that planar microwave resonators have taken on new roles: as quantum buses,[2] for generating Fock states[3] and as read-out elements for solid-state qubits.[4] Superconducting resonators are also used as kinetic-inductance detectors.[5] These applications involve measurements that need to be done quickly and accurately. It is natural to look at techniques already in use in the fields of optics and frequency metrology for inspiration on how to meet these new measurement challenges. A commonly used technique for reading-out resonators in precision frequency metrology is Pound-locking,[6,7] routinely used in quantum optics and precision frequency metrology[8] but surprisingly little known outside those fields.

The intrinsic properties of a resonator are described by its centre frequency ν_0 and unloaded quality factor $Q_u = \nu_0/\Delta\nu$, where $\Delta\nu$ is the width of the resonance. This in turn is related to the attenuation rate $\alpha = \pi\nu_0/2Q$. All these parameters are routinely measured using a vector network analyzer (VNA). Resonator measurements using a VNA are in principle accurate as long as the resonance shape is known and fitting techniques can be used to obtain Q and ν_0, but are also quite slow, only measures the average behaviour, and do not provide any direct information about the level of noise in the system. Another common approach is to use homodyne detection techniques where the carrier is mixed down to zero frequency (using a mixer).[5] Pound-locking has a few important advantages over both these methods. The main improvement comes from the fact that the modulation frequency f_m (see below) can be chosen to be much higher than the 1/f corner frequency of amplifiers, etc.; this is important since microwave amplifiers are very noisy at low offset frequencies, meaning the noise in a homodyne measurement[5,9] scheme can be easily dominated by system noise. We typically use f_m of 1–5 MHz, well above the corner frequency of our amplifiers. It is also a "real time" technique (within the bandwidth of the loop) in that it always "tracks" the centre frequency of the resonator

irrespective of the magnitude of the fluctuation, leading to a significant speedup in the measurement throughput. Finally, it also allows for accurate measurements of very small shifts in the centre frequency of a resonator which is important in many experiments.

The purpose of this paper is to describe a new application and appropriate implementation of this well-established technique. We have adapted Pound-locking to the read-out and characterization of superconducting microresonators. We will also describe how one can obtain information about the nature of the noise in samples by using analysis techniques from precision frequency metrology. It is our hope that this work will expand the applications of the Pound-locking technique.

II. POUND-LOCKING

Figure 1(a) show the basic schematic of a Pound-loop. Here, we will describe how this is implemented in the case of microwave oscillators; for a very intuitive discussion of how Pound-locking is used in optics, see the review by Black.[10] The main building blocks are a voltage-controlled oscillator (VCO) that generates a carrier of frequency f_c, a phase modulator used to add sidebands $\pm f_m$ to the signal, the resonator, a square-law power detector, a down-converting mixer, and finally a regulator circuit which controls the VCO.

The principle of operation is as follows: assuming the carrier is near resonance and the modulation frequency has been chosen so that $f_m \gg \Delta\nu$, the sidebands do not enter the resonator (note that this means that no extra power is injected into the resonator; nor is the bandwidth limited by α). The phase modulated signal going into the sample will be of the form[10]

$$V_{in} = V_0[J_0(\beta) + 2jJ_1(\beta)\sin 2\pi f_m t]e^{2\pi jf_c t}, \quad (1)$$

where $J_{0,1}$ are Bessel functions and β is the modulation depth; it can be shown that the latter should be chosen so that the power in the sidebands is -3 dB smaller than the carrier. The resonator can be anything that has a "notch" type frequency response; most Pound-loops are implemented using a circulator (meaning the sample is actually probed in reflection)

FIG. 1. (Color online) (a) The basic Pound-loop. (b) Practical implementation of the Pound-loop. Various auxiliary components (filters, etc.) have been left out for clarity.

but our planar resonator (see below and Ref. 11) have this response in transmission (see Fig. 2).

The scattering parameter S_{21} for a piece of transmission line shunted by a resonator can be written as

$$S_{21} = \frac{2(1 + 2jQ_u y)}{g + 2(1 + 2jQ_u y)}, \quad (2)$$

where g is a parameter determining the coupling strength and y is the normalized centre frequency $(f - \nu_0)/\nu_0$. After going through the sample, the signal is detected by a square-law diode after which it is demodulated using a mixer. The circuit, therefore, creates an error signal that is due to the interference between the transmitted signal and the energy leaking out from the resonator back into the transmission line. The signal from the diode can be written as[12, 13]

$$\epsilon \propto 2V_0^2 k J_0(\beta) J_1(\beta) \{ \text{Im}[S_{21}(f_c)](\text{Re}[S_{21}(f_c + f_m)]$$
$$+ \text{Re}[S_{21}(f_c - f_m)]) - \text{Re}[S_{21}(f_c)](\text{Im}[S_{21}(f_c + f_m)]$$
$$+ \text{Im}[S_{21}(f_c - f_m)]) \}, \quad (3)$$

where ϵ is the error signal, and k is a constant that depends on the conversion efficiencies of the diode and the demodulator.

The net effect of the Pound-loop is that whenever the carrier is off resonance, the transmitted signal is phase shifted

and will have an amplitude modulated (AM) component, i.e., there is partial phase modulated (PM) to AM conversion. The AM signal is then detected and used to correct the error. Hence, ideally this circuit will "lock" the frequency of the carrier f_c to the resonance frequency ν_0. Figure 3 shows what the error signal ϵ will look like for a loop with a typical resonator. Once the system has locked to the resonator, it will only undergo small excursions from ν_0 and ϵ is nearly linear; using Eq. (2) we can simplify Eq. (3)

$$\epsilon_{lin} \propto k V_0^2 \frac{4gQ_u}{(g+2)^2} y, \quad (4)$$

where we have assumed optimum modulation depth (β = 1.08). Hence, the slope of the error signal depends on the uncoupled quality factor and the coupling strength of the resonator.

III. EXPERIMENTAL

The actual setup used in our experiment can be seen in Fig. 1(b). Our resonators are thin-film devices

FIG. 2. (Color online) Micrograph and equivalent circuit for one of our lumped element resonators. The electromagnetic radiation is primarily inductively coupled to the inductive part of the resonator. The coupling strength is set by the mutual inductance between the coplanar transmission line and the resonator.

FIG. 3. (Color online) Simulated typical error signal. The parameters are f_m = $\nu_0/2000$, $Q = 50\,000$, $g = 2$, and $\beta = 1.08$.

microfabricated on 5×10 mm^2 chips (see Ref. 11 for a full description). The chip is glued to a copper cold-finger and bonded to a connectorized chip carrier which is enclosed in an aluminium box; the box is then mounted on the mixing chamber of a dilution fridge which has a base temperature of 30 mK. The in-signal to the resonator goes via a filtered and heavily attenuated (50 dB) line. The out-signal passes through an isolator and then into a low-noise cryogenic amplifier with a noise temperature of about 4 K.

The microwave signal (hereon referred to as the carrier) is generated by a voltage-controlled oscillator; in practice, this is usually a microwave generator where the output frequency can be modulated using an external voltage (at a rate of, for example, 10 kHz/V). Another option is to use a local oscillator (LO) held at a fixed frequency and mix it with an intermediate frequency (IF) from a low-frequency VCO (in practice, e.g., a function generator that can be frequency modulated) using, for example, a single-sideband modulator. The performance of the latter setup is in principle better since a low phase-noise LO can be used (the phase noise of the IF source is negligible) but makes the circuit more complicated (and care has to be taken to minimize the amplitude of the sidebands). Another advantage of this latter arrangement is that the frequency shift can be read out directly with high accuracy using a standard counter. The carrier then passes through a phase modulator which adds sidebands $\pm f_m$. The shape of the error signal depends on the phase of the modulating signal, so this needs to be adjusted to compensate for lead/lag caused by the cables, filters, etc. The signal from the diode then goes to an RF lock-in amplifier (referenced to f_m) which is used with a very short time constant (as to not limit the bandwidth of the loop), essentially being operated as a mixer with gain. The error signal in the loop is the in-phase signal from the lock-in amplifier, and is fed to the proportional integral differential (PID) controller. The output voltage from the controller then controls the VCO (which in our case outputs the IF) in order to null the error; we generally use a deviation of 5–100 kHz/V. The PID controller is configured so that it attempts to keep the error signal as close to zero as possible while still maintaining a loop bandwidth much larger than the frequency range of any noise we want to study. Care has to be taken to avoid dependence of the observed noise level on the loop parameters; this can happen, e.g., if the gain is too high (resulting in oscillations that distort the noise spectrum) or the bandwidth is too low (resulting in a roll-off of the noise at higher frequencies).

Most of our measurement data are acquired using a standard 16-bit data acquisition system connected to the output of the PID controller. Sampling rates from 10 Hz to about 50 kHz are used, depending on the measurement time which varies from a few seconds to tens of hours. We also monitor the output signal using an FFT analyzer. In order to get an independent measure of the frequency, we monitor the frequency of the IF source using a separate counter. All microwave equipments, counters, etc., in our experiment use an external 10 MHz frequency reference derived from a hydrogen maser. Our current setup allows us to track any change to the resonance frequency of the resonator with a bandwidth of a few kHz (limited by the PID controller) and a "real-time"

frequency resolution of a few parts in 10^8 (limited by the intrinsic noise of the resonator).

Our experiment is essentially dual to that of the conventional setup used to improve the stability of an oscillator. In a conventional experiment, a "bad" oscillator is locked to a "good" resonator; we are here doing the exact opposite. The frequency noise level of our resonator is much higher than that of the carrier; by observing how the circuit strives to null the error signal, we obtain direct information about the resonator. Moreover, since we are operating at offset frequencies smaller than $f_L = \nu_0/2Q$ ($\sim$75 kHz), the Leeson effect[8] will not affect the shape of the frequency spectrum.[14]

Our superconducting planar lumped element (LE) resonators are about 300×300 μm^2 in size, fabricated from niobium on a sapphire substrate. Several resonators (usually 5) are fabricated on the same chip and are coupled to the same transmission line allowing for frequency multiplexing. The data shown here come from a resonator with ν_0 of 7.5 GHz and a loaded $Q = 50\,000$, it is similar to the ones discussed in Ref. 11. Here, we only show a subset of our results; for a full discussion, see Ref. 15.

In order to verify that our data really represent properties of the sample and are not measurement artifacts, we also employ a number of reference samples. Here, we will, therefore, also show data from a common dielectric resonator (DRO) in the shape of a "puck" about 7 mm in diameter mounted inside a metal box and measured at room temperature. In this experiment, we locked to a mode with a resonance frequency of 5.12 GHz and a loaded $Q = 5500$.

IV. DATA ANALYSIS

The most straightforward way to measure noise is to use a spectrum analyzer or – equivalently – to calculate the power spectral density (PSD) from sampled time-domain data. Figure 5 shows a typical PSD from one of our LE resonators. Note that what is plotted is the frequency noise (in units of Hz/$\sqrt{\text{Hz}}$) meaning the PSD represent spectral information of how the centre frequency of the resonator changes.

The spectrum shows that random walk frequency noise (slope -1) dominates at low frequencies but that processes with a white (slope 0) spectra gradually takes over as the frequency increases. The solid line with slope -0.5 can be identified with flicker frequency noise.

One limitation of PSD is that it is often very difficult to analyze "slow" processes. Another little known, but highly useful tool from the arsenal of frequency metrology is the Allan deviation (ADEV).[16, 17] Here, we have used the overlapping Allan deviation σ

$$\sigma^2 = \frac{1}{2m^2(M-2m+1)} \sum_{j=1}^{M-2m+1} \left\{ \sum_{i=j}^{j+m-1} (\overline{y}_{i+m} - \overline{y}_i) \right\}^2,$$
(5)

where M is the number of samples, τ_0 is the measurement timebase, and $\overline{y}$ is the time-averaged fractional frequency. ADEV is the most common measure of time-domain stability, but other related types of measures such as the modified Allan deviation (MDEV) and Hadamard deviation are also very

TABLE I. Noise processes and the resulting slope in the root PSD and Allen deviation (ADEV) plots.

Noise type	Root PSD slope	ADEV slope
White phase	1	−1
Flicker Phase	0.5	−1
White frequency	0	−0.5
Flicker frequency	−0.5	0
Random walk	−1	0.5
Linear drift	. . .	1

useful for analyzing and identifying noise (e.g., the MDEV in particular can distinguish between white and flicker phase noise). Using the Allan deviation, it is relatively easy to identify noise processes that happen over a long timescale. Just as in the case of the PSD, we categorize the noise depending on the slope of the curve[16] when plotted in a log-log plot. Table I shows a summary. Note that we have included frequency drift in Table I, although strictly speaking not a type of noise, drift due to, e.g., temperature fluctuations are often seen in real measurements.

In order to demonstrate how ADEV can be used to analyze the intrinsic noise of resonators, we first show the experimental data from the DRO in Figure 4.

White frequency noise (slope −0.5) dominates as expected for short times until linear drift (slope +1) takes over and the deviation increases rapidly. This large drift in the resonance frequency (about 10–20 Hz/s)is due to a changing temperature and agrees with the specified temperature stability of a few ppm/K. By employing some rudimentary temperature stabilization, we can shift the onset of the drift further to the right on the plot. According to this plot, the best one can hope for is a short term stability (and read-out accuracy δf) of about 0.2 Hz, which agrees with the white noise level measured using an FFT analyzer as well as the direct read-out using a counter. This corresponds to a line splitting factor $\Delta \nu / \delta f$ of 5×10^6. Figure 5 shows the ADEV – calculated using the same dataset as was used for the PSD – for the lumped element resonator measured at 30 mK. It is quite clear that the behavior is very different from that of the dielectric resonator. Flicker frequency noise (slope 0) dominates at both long and short timescales, but the dominant feature is the sudden rise at timescales between 1 ms and 1 s. We attribute this to ran-
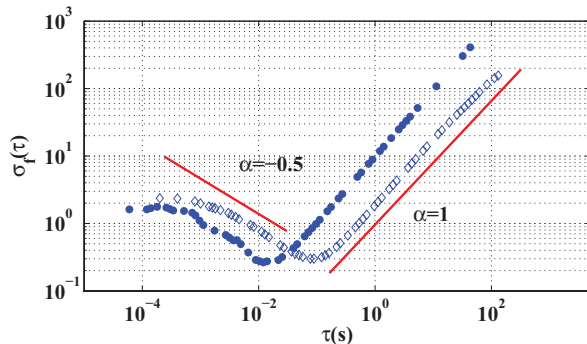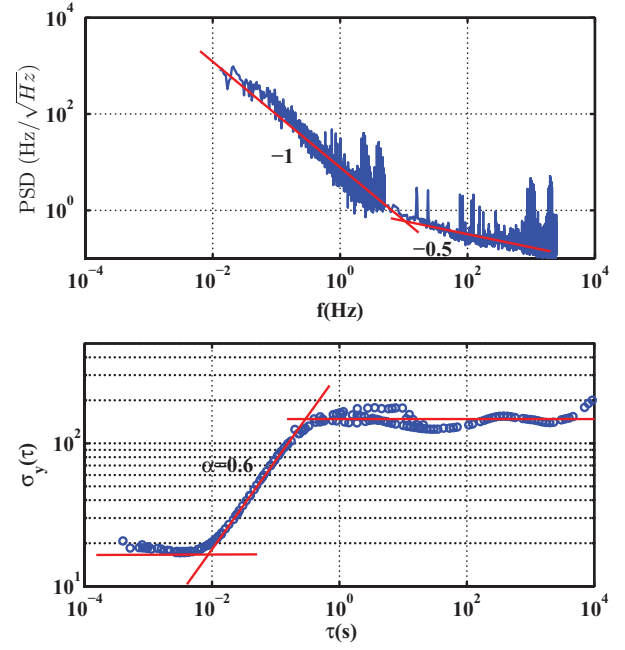

FIG. 5. (Color online)Top: Root power spectral density (in units of $Hz/\sqrt{Hz}$) for a 7.5 GHz lumped element resonator measured at 30 mK. the solid lines have a slope of −1 and −0.5, respectively and are meant as guides for the eye. The PSD was calculated using a zoom FFT algorithm with a Hanning window. Bottom: Allan deviation plot for a 7.5 GHz lumped element resonator measured at 30 mK. The power in the resonator is approximately −100 dBm.

dom walk noise (slope 0.5). It is interesting to compare this with the PSD. One obvious difference is that we in the ADEV can now distinguish the types of noise much more easily. The random walk noise – which is the most prominent feature in Fig. 5 – is quite difficult to distinguish from other types of noise in the PSD and the ADEV also makes it easier to see over which timescale a particular noise process dominates. Another advantage of the Allan deviation is that it is less susceptible to numerical artifacts than spectral methods, i.e., it does not suffer from problems similar to the un-normalizable pole at the origin of a PSD, nor is a window function needed.

Note that the line splitting factor at long times for the LE resonator is about 1500, much worse than for the dielectric resonator. This is simply a consequence of the fact that the LE resonator is – despite having a much higher Q – much worse at stabilizing the Pound-loop. This in turn can be attributed to the fact that the LE resonator is subject to noise from its environment: the flicker frequency noise is most likely due to the presence of two-level fluctuators;[5] the random walk noise might be due to random changes in the dielectric environment (due to hopping) or the movement of trapped vortices in the superconducting film.

V. CONCLUSION

By bringing well-known measurement techniques and analysis methods from time and frequency metrology to bear on the problem of the nature of noise in superconducting resonators, one can gain a lot of information not readily obtainable using more widely known techniques. By implementing a Pound-loop and analyzing the data using the Allan deviation, we are able to identify noise processes that are hard

FIG. 4. (Color online) Allan deviation plot for the dielectric resonator, with(diamonds) and without(points) temperature stabilisation.

to distinguish by conventional means. Moreover, the fact that the loop directly measures the resonance frequency makes the analysis more straightforward. Finally, we would also like to mention that the ability to "track" the value of ν_0 can also lead to significant improvement in measurement throughput. A good example is measurements of ν_0 vs. temperature which can, e.g., be used to determine the intrinsic loss tangent due to two-level fluctuators in the sample. This can be a time-consuming process, if one needs to "step" the temperature and wait for it to stabilize before acquiring the scattering parameters (S21 and/or S11) using a VNA. However, by using a Pound loop, one is only limited by the thermal time-constant between the sample and the temperature sensor, allowing for the temperature to be ramped relatively quickly.

ACKNOWLEDGMENTS

[1] C. C. Gerry and P. L. Knight, *Introductory Quantum Optics* (Cambridge University Press, Cambridge, England, 2005).

[2] M. A. Sillanpaa, J. I. Park, and R. W. Simmonds, Nature (London) **449**, 438 (2007).

[3] M. Hofheinz, E. M. Weig, M. Ansmann, R. C. Bialczak, E. Lucero, M. Neeley, A. D. O'Connell, H. Wang, J. M. Martinis, and A. N. Cleland, Nature (London) **454**, 310 (2008),

[4] A. Wallraff, D. Schuster, A. Blais, L. Frunzio, R. Huang, J. Majer, S. Kumar, S. Girvin, and R. Schoelkopf, Nature (London) **431**, 162 (2004).

[5] J. Gao, J. Zmuidzinas, B. A. Mazin, H. G. LeDuc, and P. K. Day, Appl. Phys. Lett. **90**, 102507 (2007).

[6] R. Pound, Rev. Sci. Instrum. **17**, 490 (1946).

[7] R. Drever, Appl. Phys. B **31**, 97 (1983).

[8] E. Rubiola, *Phase Noise and Frequency Stability in Oscillators* (Cambridge University Press, Cambridge, England, 2009).

[9] R. Barends, H. L. Hortensius, T. Zijlstra, J. J. A. Baselmans, S. J. C. Yates, J. R. Gao, and T. M. Klapwijk, IEEE Trans. Appl. Supercond. **19**, 936 (2009).

[10] E. D. Black, Am. J. Phys. **69**, 79 (2001),

[11] T. Lindström, J. E. Healey, M. S. Colclough, C. M. Muirhead, and A. Y. Tzalenchuk, Phys. Rev. B **80**, 132501 (2009).

[12] J. Anstie, Ph.D. dissertation, University of Western Australia, 2006.

[13] S. Chang, Ph.D. dissertation, University of Western Australia, 2000.

[14] E. Rubiola, private communication (31 May 2011).

[15] T. Lindström, J. Burnett, M. Oxborrow, and A. Y. Tzalenchuk, "Frequency stability of superconducting microresonators" (unpublished).

[16] W. Riley, NIST, Tech. Rep. 1065, 2008.

[17] T. Witt and D. Reymann, IEE Proc.: Sci., Meas. Technol. **147**, 177 (2000).